• Clinical Research •

Assessment of optic nerve and optic tract alterations in patients with orbital space-occupying lesions using probabilistic diffusion tractography

Chun-Nan Wu[1,2], Shao-Feng Duan[3,4], Xue-Tao Mu[2], Yi Wang[5], Peng-Yu Lan[2], Xiao-Lu Wang[6], Kun-Cheng Li[1]

[1]Department of Radiology, Xuanwu Hospital, Capital Medical University, Beijing 100053, China
[2]Department of Radiology, the Third Medical Center of Chinese PLA General Hospital, Beijing 100039, China
[3]Division of Nuclear Technology and Applications, Institute of High Energy Physics, Chinese Academy of Sciences, Beijing 100049, China
[4]Beijing Engineering Research Center of Radiographic Techniques and Equipment, Beijing 100049, China
[5]Orbital Disease Institute, the Third Medical Center of Chinese PLA General Hospital, Beijing 100039, China
[6]Department of Otolaryngology, the Third Medical Center of Chinese PLA General Hospital, Beijing 100039, China
Correspondence to: Kun-Cheng Li. Department of Radiology, Xuanwu Hospital, Capital Medical University, Beijing 100053, China. cjr.likuncheng@vip.163.com
Received: 2018-08-15 Accepted: 2019-05-15

Abstract
● **AIM: To investigate the diffusion changes in both the optic nerve and optic tract in orbital space-occupying lesion patients with decreased visual acuity, and its clinical significance using probabilistic diffusion tractography (PDT).**

● **METHODS: Twenty patients with orbital space-occupying lesions and 25 age- and gender-matched healthy persons were included. All patients and controls underwent routine orbital magnetic resonance imaging and diffusion tensor imaging (DTI), using a 3.0T magnetic resonance scanner (Trio Tim Siemens). After the image data were preprocessed, each DTI parameters of the optic nerve and optic tract was obtained by PDT, including fractional anisotropy (FA), mean diffusivity (MD), axial diffusivity (AD) and radial diffusivity (RD). The asymmetry index (AI) of each parameter was calculated. Compared the parameters of the affected side optic nerve and ipsilateral optic tract with the contralateral side by paired sample *t*-test; compared AI of parameters of optic nerve and optic tract between the patient group and the control group by independent sample *t*-test. Patients were divided into three subgroups according to the low vision grade standard of WHO, compared the FA and AI of FA between the three subgroups by single factor variance analysis.**

● **RESULTS: The affected side optic nerve presented significantly decreased FA, increased MD, AD, and RD values compared to the unaffected side (P<0.05). The AI of FA, MD, AD, and RD of optic nerve in the patients was significantly higher than that of the controls (P<0.05). The comparison results of the optic tract showed that there was no significant difference between the patient group and control group in terms of the bilateral optic tracts in patients (P>0.05). The AIs of the FA value of the optic nerve in the eyesight <0.1 subgroup was significantly higher than that in the other groups (P<0.05).**

● **CONCLUSION: FA, MD, AD, and RD of the affected side optic nerve of the orbital space-occupying lesions have significantly changed, the FA value is the most sensitive. The PDT could be a useful tool to provide valid quantitative markers of optic nerve injuries and evaluate the severity of orbital diseases, which other examinations cannot be acquired.**

● **KEYWORDS:** orbital space-occupying lesions; decreased vision; optic never and optic tract; probabilistic diffusion tractography; magnetic resonance imaging

DOI:10.18240/ijo.2019.08.11

Citation: Wu CN, Duan SF, Mu XT, Wang Y, Lan PY, Wang XL, Li KC. Assessment of optic nerve and optic tract alterations in patients with orbital space-occupying lesions using probabilistic diffusion tractography. *Int J Ophthalmol* 2019;12(8):1304-1310

INTRODUCTION

The diminution of vision, especially vision deprivation, can seriously affect the quality of human life. Orbital space-occupying lesions are one of the important causes of visual acuity decreases, especially those that occur at the orbital apex or around the optic nerve, which compress or even damage the optic nerve, thus causing vision loss or visual deprivation. At present, ophthalmologists typically utilize the ophthalmoscope, the visual evoked potential (VEP) and the visual chart test to evaluate patients' vision in clinics, but ocular fundus examinations can only show the condition of the fundus oculi and papilla. Meanwhile, the results of the VEP and vision test can contain certain error, and these examinations cannot assess optic nerve damage quantitatively. Magnetic resonance imaging (MRI) plays a critical role in the diagnosis and differential diagnosis of orbital space-occupying lesions, and it can display the morphology and signal characteristics of the lesion distinctly[1], but the conventional MRI cannot quantitatively analyze the pathological changes in the fibers of the visual pathway. Diffusion tensor imaging (DTI) shows the shape and structure of white matter fiber bundles *in vivo* and simultaneously obtains several parameters that can reflect the alterations in the microstructure of fiber bundles[2-5]. Hence, DTI provides the possibility for early quantitative detection of the fiber damage conditions in the visual pathway.

DTI has been applied for the quantitative evaluation of changes in visual pathway fibers concerning glaucoma, neuromyelitis optica, optic neuritis, amblyopia, and several other ophthalmic diseases, but no DTI study has studied the visual pathway of orbital space-occupying lesions[6-8]. Therefore, this research group attempted to quantitatively assess the severity of optic nerve injuries and even whole visual pathways in patients with orbital space-occupying lesions using DTI to help clinicians determine the severity of the illnesses and establish treatment plans. In this study, the quantitative analysis of DTI was carried out using probabilistic diffusion tractography (PDT). PDT is a post-processing analysis method that is applied after obtaining clinical conventional DTI data. PDT is different from the analysis method used in previous studies[9-11]. The latter usually selects one region of interest (ROI) or the average value of three ROIs to determine the parameter value, which makes it easy to generate measurement error. The parameter value obtained by PDT represents the average value of the whole region of the interest. For example, the parameter value of the optic nerve represents the entire optic nerve region rather than a certain point. Therefore, the results that obtained are more accurate and objective. Studies have reported that PDT is superior to deterministic tractography technology in evaluating the microstructure of white matter fiber bundles[12-13].

Our study uses the asymmetry index (AI) for comparative analysis. The AI refers to the asymmetry of the parameter values between left and right sides. In the normal control group, the AI represents the asymmetry of the parameter values between the left and right sides, while, in the patient group, the AI represents the asymmetry between the affected side and the normal side. The higher the AI value is, the more asymmetrical the two sides are.

DTI has been used in the study of optic nerve fiber bundles, including those of normal people, animal models and patients with ophthalmic diseases[14-17]. Sidek *et al*[18] reported that fractional anisotropy (FA) decreased and that mean diffusivity (MD) increased in the optic nerve and optic radiations of patients with severe glaucoma using DTI. Most of the literature reports on the optic nerve and optic radiations using DTI studies, and few studies on the optic tracts of normal people or patients use DTI[19-20]. To our knowledge, we are the first report to quantitatively analyze the optic nerve and optic tract changes caused by orbital lesions using PDT technology, and assess the value of DTI parameters in revealing the integrity of visual pathway fibers and pathological changes in orbital diseases.

SUBJECTS AND METHODS

Ethical Approval The study was conducted in accordance with the Declaration of Helsinki and was approved by the Research Ethics Committee of Xuanwu Hospital of Capital Medical University and the Third Medical Center of Chinese PLA General Hospital. All patients had been fully informed of the purpose and methods of the present study and provided written informed consent from themselves or their guardians.

Subjects A total of 20 patients (8 females and 12 males; mean age, 41.6±12.7y; range, 18-68y) with unilateral orbital space-occupying lesions were enrolled during a 12-month period in our institution. The inclusion criteria of the patient group included the following: unilateral orbital space-occupying lesions associated with decreased vision, as certified by a visual chart test; no other eye diseases, such as glaucoma or inflammatory lesions of the visual pathway; and no craniocerebral space-occupying lesions. Meanwhile, 25 normal volunteers [13 males and 12 females; (mean age, 38.6±12.6y, range, 23-61y)] were included in the control group. The inclusion criteria of the control group were as follows: except for myopia, the ophthalmological examination was normal; the exclusion of inflammatory diseases of visual pathways and no history of head trauma; a normal finding from the conventional MRI of the brain, especially the visual pathway region; and no history of psychoactive drug or hormone usage.

Data Acquisition The MRI examinations were performed on a 3.0T MRI imaging system (Trio Tim Siemens, Germany) with an 8-channel head coil. Head motions were minimized with restraining foam pads. During the scanning process, patients and volunteers were asked to close their eyes gently and refrain from moving their eyeballs to minimize the effects of deliberate eye movement during the acquisition time.

All patients and the control group underwent routine orbital MRI and DTI. The routine orbital MRI examination included a pre-enhanced T1-weighted image (T1WI) and T2-weighted image (T2WI) in the axial and coronal planes and a post-enhanced T1WI with frequency-selective fat saturation in the axial, coronal, and sagittal planes. The imaging parameters were as follows: T1WI, repetition time/echo time (TR/TE)=200ms/2.46ms; angle=70°; T2WI, TR/TE=3400ms/108ms; angle=120°; FOV=190×190 mm^2;

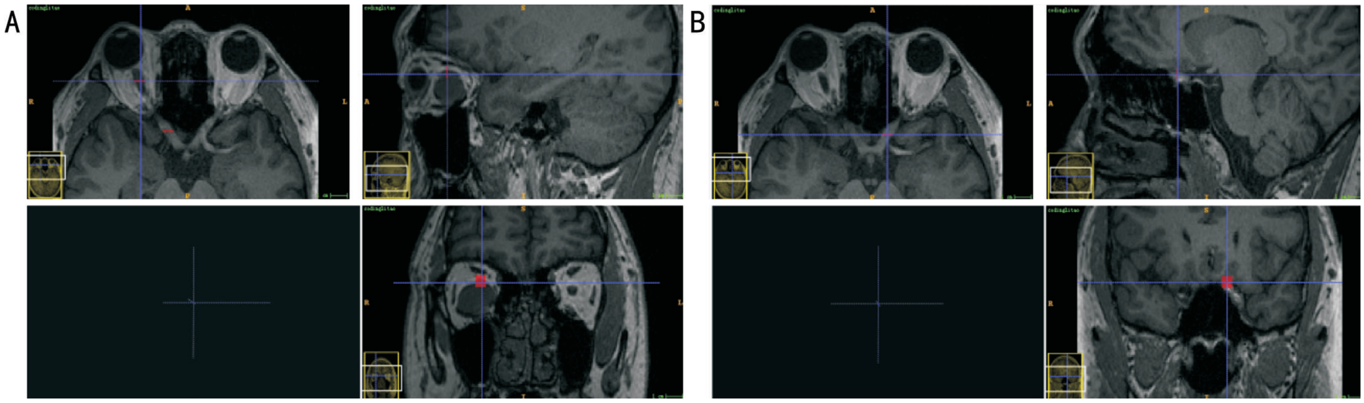

Figure 1 Positioned seed mask on the optic nerve A: Two seed masks at the near and far segment of the affected side optic nerve. B: One seed mask at the near segment of the normal side optic nerve.

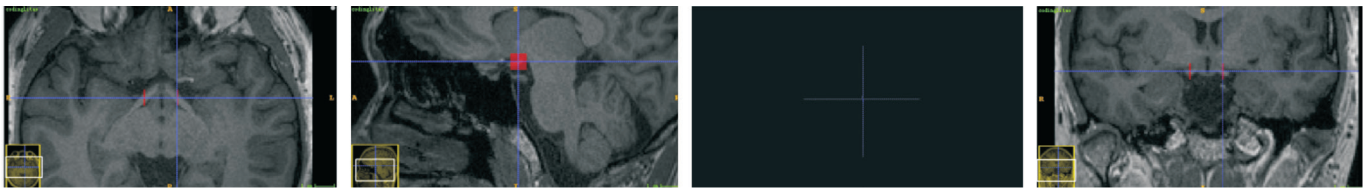

Figure 2 Positioned seed mask on the optic tract Located on the optic tract pathways in the sagittal plane, one seed mask consisting of 9 voxels was selected and positioned at the middle segment of the double lateral optic tract.

matrix=256×256; slice thickness=3 mm; and slice gap=0.3 mm. Gd-DTPA (Magnevist, Bayer HealthCare, Berlin, Germany) was injected intravenously into the elbow vein at a dose of 0.2 mL/kg and flow rate of 3 mL/s.

DTI was conducted on each subject with a single-shot echo planar imaging (EPI) diffusion tensor sequence, which covered the whole visual pathway. The specific parameters were as follows: TR=8300ms, TE=91ms, FOV=220×220 mm^2, matrix=128×128, number of signal averages=4, slice thickness=2.0 mm, b b=0 and 1000s/mm^2, and the scanning time was 12min and 4s. The anatomical data were obtained in a T1-weighted 3D-MPRAGE sequence (TR=1900ms, TE=2.58ms, FOV=240×240 mm^2, matrix=256×256, and reconstructed axial plans with 1.2-mm slice thickness). All the axial data were acquired on an oblique axial plane parallel to the anterior commissure-posterior commissure (AC-PC) line.

Data Preprocessing Every subject had a dataset consisting of 21×4 volumes. For each dataset, the effects of the head motion and distortion induced by the eddy current were corrected by FMRIB'S diffusion toolbox (FDT), which is a part of the FSL (FMRIB Software Library, FSL, Britain). Then, the corrected datasets were split into four datasets that corresponded to four DTI scans. Next, the four datasets were averaged to generate a mean DTI dataset to reduce noise. Finally, the mean DTI dataset of each subject was modeled using DTIFIT to produce the FA, mean diffusivity (MD), radial diffusivity (RD) and axial diffusivity (AD) images.

Probabilistic Tractography Before the probabilistic tractography, we used BEDPOSTX with the default options to estimate the fiber orientation within each voxel. Subsequently,

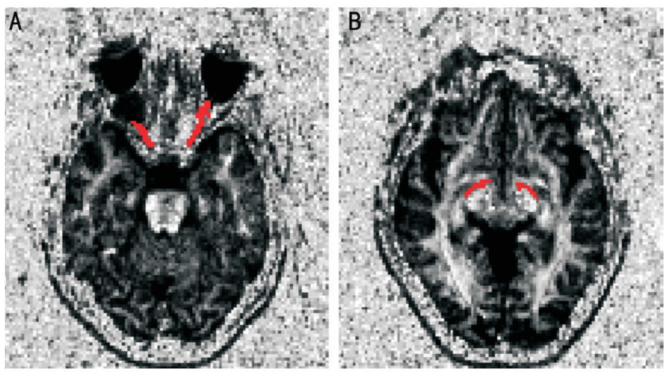

Figure 3 The fiber bundle imaging was obtained using the probabilistic fiber bundle tracking technique A: Bilateral optic nerve; B: Bilateral optic tract.

the tractography was run using PROBTRACKX with the following basic parameters: the number of samples was 5000, the curvature threshold was 0.2, a single mask used as the seed to extract the target tracts, and other exclusion masks were generated to prohibit the tracking of the wrong pathways. All seed masks were initially drawn on the anatomical images, which was followed by a transformation to the diffusion space using the deformation field derived from registering the T1 image to the FA image. For the optic nerve, a seed mask consisting of 7 voxels was positioned in the pathway of the optic nerve at the coronal slice (Figure 1). For the optic tract, a seed mask consisting of 9 voxels was positioned in the pathway of the optic tract at the sagittal slice (Figure 2). Connectivity distributions were generated from each voxel in the seed mask, and thresholds were set to include only those pathways that exhibited a probability of >10% (Figure 3). For each tract, the mean FA, MD, RD, and AD were determined.

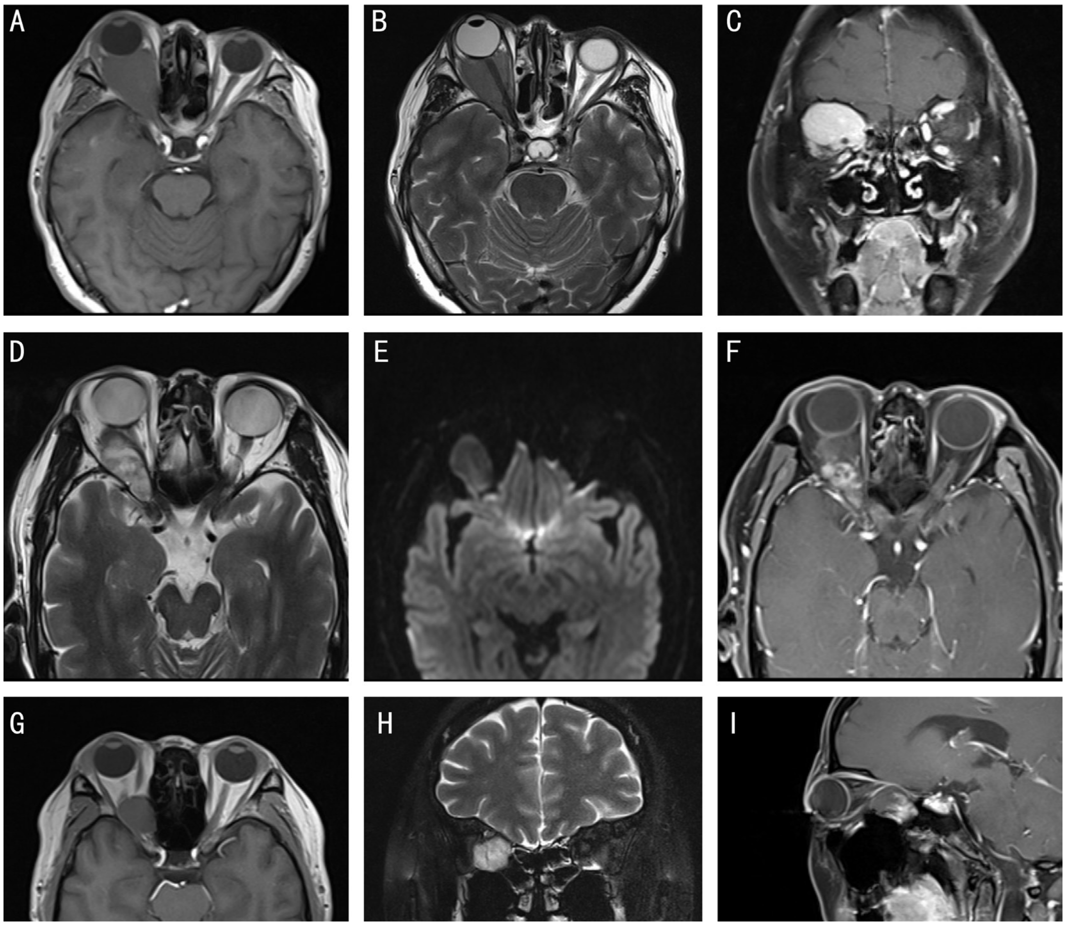

Figure 4 Optic nerve changes caused by orbital space-occupying lesions A-C: For the same respective cases, the T1WI, T2WI, and fat saturation enhancement scan images on the body axis transection showed the optic nerve sheath meningioma growth surrounding the right orbital optic nerve, and the enhanced scan images also showed the optic track sign. D-F: For the same respective cases, the T2WI, DWI, and fat saturation enhancement scan images of the body axis transection showed displacement and compression of the right orbit optic nerve, cyst degeneration was seen in the lesions, and the pathological diagnosis was schwannoma. G-I: For the same respective cases, the body axis of the cross-sectional T1WI, coronary fat saturation T2WI, and sagittal fat saturation enhancement scan images showed the right orbitofrontal optic nerve compression that obviously attenuated and shifted the position and diagnosis of the cavernous hemangioma by pathological examination.

Statistical Analysis We conducted two kinds of comparisons for the optic nerves and optic tracts using SPSS version 22.0 (SPSS, IBM Co., Armonk, NY, USA). First, we compared the affected side optic nerve and ipsilateral optic tract with the contralateral side to determine whether the differences in DTI parameters (FA, MD, RD and AD) between the bilateral parameters were statistically significant by paired sample *t*-test. Second, the AI values of various parameters (FA, MD, RD and AD) of the optic nerve and optic tract were compared between the patient group and the control group. Here, AI=(right parameter value−left parameter value)/(right value+left value). The difference in AIs between the two groups was analyzed by an independent sample *t*-test. Third, according to the WHO classification standard of low vision, patients were divided into three subgroups: vision>0.3, vision between 0.3-0.1 and vision<0.1 (including no light sensation). We adopted a single factor variance analysis to compare the difference between the FA value and the AI of the FA among the three groups. All the above statistical analyses took the statistically significant threshold value of $P<0.05$.

RESULTS

Routine Magnetic Resonance Imaging There was no significant difference in age or gender between the patient group and the control group. All cases were confirmed by pathological examination, including nine cavernous hemangiomas, three lymphomas and optic nerve sheath meningiomas, one schwannoma, one diffuse proliferation of the lymphoid tissue, one lymphangio-hemangioma, one hemangioblastoma, and one inflammatory pseudotumor. The optic nerve was compressed or encompassed by a tumor or neoplasm, thus resulting in optic nerve displacement, thinning and even unclear displays (Figure 4). There was no abnormality observed in the morphology or signal of the optic nerve and optic tract in the normal control group.

Differences Between the Bilateral Optic Nerves and Optic Tracts in the Patient Group The affected side optic nerve

Table 1 Comparison of the DTI parameters between the bilateral optic nerve and optic tract in the patient group

Parameters	Optic nerve				Optic tract			
	Affected side	Normal side	*t*	*P*	Affected side	Normal side	*t*	*P*
FA	0.276±0.044	0.383±0.112	-4.404	0.000	0.338±0.050	0.355±0.108	-0.763	0.455
MD	1.094±0.182	0.853±0.273	2.999	0.007	1.244±0.168	1.240±0.372	0.044	0.966
AD	1.365±0.212	1.113±0.332	2.585	0.018	1.643±0.182	1.644±0.329	-0.027	0.979
RD	0.959±0.171	0.728±0.238	3.323	0.004	1.044±0.167	1.038±0.397	0.072	0.943

DTI: Diffusion tensor imaging; FA: Fractional anisotropy, MD: Mean diffusivity, AD: Axial diffusivity; RD: Radial diffusivity (MD value, AD, RD)×10^{-3} mm/s.

Table 2 Comparison of the AIs for the DTI parameters of the optic nerve and optic tract between the control and patient groups

Parameters	Optic nerve				Optic tract			
	Patient group	Control group	*F*	*P*	Patient group	Control group	*F*	*P*
AI of FA	0.149±0.121	0.077±0.051	12.928	0.000	0.126±0.125	0.093±0.134	0.209	0.325
AI of MD	0.175±0.201	0.100±0.797	3.297	0.038	0.099±0.075	0.057±0.068	0.552	0.231
AI of AD	0.156±0.199	0.085±0.069	3.095	0.043	0.069±0.047	0.046±0.058	0.393	0.267
AI of RD	0.183±0.187	0.114±0.089	3.483	0.035	0.129±0.095	0.069±0.078	1.161	0.144

AI: Asymmetry index; DTI: Diffusion tensor imaging; FA: Fractional anisotropy, MD: Mean diffusivity, AD: Axial diffusivity, RD: Radial diffusivity.

presented significantly decreased FA, increased MD, AD, and RD values compared to the unaffected side (*P*<0.05). The FA value displayed a very significant difference (*P*<0.001). No significant differences were observed in the optic tract between the same side with the lesion and the contralateral side (*P*>0.05; Table 1).

Differences of AI values of the Optic Nerve and Optic Tract Between the Patient Group and the Control Group The AI of FA, MD, AD, and RD of optic nerve in the patients was significantly higher than that of the controls (*P*<0.05). Among them, the AI of the FA showed the highest significant difference (*P*<0.001). There was no significant difference in all the AIs of the parameters of the optic tract between the patient group and the control group (*P*>0.05; Table 2).

Differences of the FA Value and AI of FA in the Affected Side Optic Nerve Between Three Subgroups There was no significant difference (*P*>0.05) in the FA values of the affected side optic nerve among the three subgroups, but the difference in the AI of the FA was significant (*P*<0.05). The AI of the FA in the eyesight <0.1 subgroup was significantly higher than that in the other groups (Figure 5).

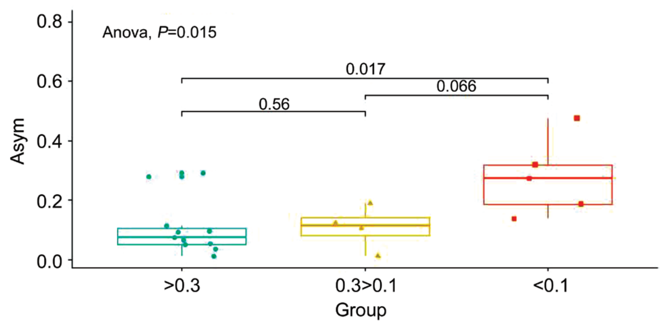

Figure 5 Comparison of the AI of the FA of the optic nerve in different eyesight subgroups.

DISCUSSION

This research adopts the PDT technique for the extraction of nerve fiber bundles, and PDT was first proposed in 2003 by Behrens *et al*[21]. The PDT method estimates the uncertainty of the voxel's diffusion tensor first and then samples the probability according to the estimated results, acquiring the tracking information of the next voxel and repeating the above process to generate many samples of fiber structure; thus, it can obtain the connection probability between the seed point and the whole target area[21-22]. This technology can evaluate all the spatial distribution of white matter fibers from a seed point, and, even when the possibility of a direction branch is very low, it still can continue to track the tractography. Therefore, this method is thought to be a reliable tool for tracking small and complex fibers, and it especially has a better effect when tracking cross fibers[23]. Compared with the deterministic tractography, the PDT can describe the morphology and structure of the brain white matter fiber bundle more accurately[24]. Due to its better noise immunity and better effect in tracking cross fiber bundles, the PDT is helpful in reducing the influence on DTI imaging by reason of the correlation of the optic fiber and the orbital structure condition. In addition, the data in this study were obtained from routine clinical DTI scanning, and the scan time was approximately 12min. Therefore, patients were more likely to accept the procedure, and the procedure has great potential for clinical applications.

Our study found that the FA values of optic nerves on the affected side were significantly lower than those on the unaffected side, and the MD values of the optic nerves on the affected side were significantly higher than those on the unaffected side. Because different eigenvalue combinations can generate the same FA values, the AD and RD play equally important roles in reflecting the demyelination and axon damage of fiber bundles[15-16,25]. The AD and RD reflect the diffusion characteristics of water molecules parallel and perpendicular, respectively, to the fiber bundle, which can distinguish the axons and myelin damage to some extent. The increase in the RD reflects the loss of myelin, and the increase in the AD reflects the degeneration of axons[15,26]. Herein, we found that both the AD and RD values of optic nerves on the affected side were higher than those on the normal side. Therefore, the author speculated that the affected side optic nerve had both axonal degeneration and myelin sheath damage.

AI has been widely used in many professional studies, such as those of hemispheric brain asymmetry differences in youths with attention-deficit/hyperactivity disorder, a robust cerebral asymmetry in the infant brain, and facial plastic research[27-29]. In this study, AI was used as the comparison index between the patient group and the healthy control group. When the parameter values of the affected side optic nerve changed, the asymmetry increased between the bilateral parameter values. Our results found that the asymmetry of both sides of the patient group was greater than that of the control group.

This study found that both the comparison of each parameter value and the comparison of the AI, FA value and AI of the FA value had the most significant differences ($P<0.001$), thus the result suggested that the FA value is the most sensitive. On the basis of above results we suggest that PDT could be useful for quantifying optic nerve damage of the orbital space-occupying lesions and evaluate the severity levels of the disease.

Several studies reported that significant differences were found in the FA, MD, AD, and RD of the optic nerve and optic radiation in glaucoma, thus indicating that glaucoma affects intracranial visual pathway fibers[8,10,18]. The results of our study showed that there was no abnormal change in the DTI parameter values of optic tracts on both the ipsilateral and contralateral sides, and there was no significant difference in the AI values of each parameter between the patient group and the control group either. It was speculated that orbital space-occupying lesions with decreased vision only damaged the optic nerve but did not change the optic tract significantly.

According to the WHO classification standard of low vision, patients were divided into three subgroups, and the results found that the FA values of the affected side optic nerves were similar between groups, which was similar to a DTI study on subacute anterior ischemic optic neuropathy[9]. However, there was a significant difference in the AI values of the FAs among the three groups in this study. The AI value of the lowest eyesight group was the highest. The author believes that the AI value of the FA of the optic nerve is associated with the severity of visual impairment. In the future, the sample size will be enlarged to further confirm this view.

As preliminary research of orbital space-occupying lesions, this study has the following limitations. First, the relatively small sample size resulted in a lack of ability to group the patients in a more detailed manner, according to different diseases. Second, this study is a horizontal study. If the longitudinal follow-up of the enrolled patients can be completed, this can provide more convincing evidence.

In conclusion, PDT technology was used for the first time to evaluate the optic nerves and optic tracts quantitatively in orbital space-occupying lesions with decreased vision in this study. The affected side optic nerve presented significantly decreased FA, increased MD, AD, and RD values, while no significant alterations were observed in the optic tract. And that FA value is the most sensitive. The severity of visual acuity decreased was assosiated with the FA value of the optic nerve. We consider that PDT can provide valid indicators to evaluate the impairment of optic nerve, the curative effect and the prognosis for clinicians, which other examinations can not acquired. Furthermore, this method may even be used to judge whether the degeneration/damage of the optic nerve is reversible or not.

ACKNOWLEDGEMENTS

Foundations: Supported by the National Natural Science Foundation of China (No.81471649); Beijing Municipal Science and Technology Commission (No. Z171100000117001).

Conflicts of Interest: Wu CN, None; **Duan SF,** None; **Mu XT,** None; **Wang Y,** None; **Lan PY,** None; **Wang XL,** None; **Li KC,** None.

REFERENCES

1 Razek AA, Elkhamary S, Mousa A. Differentiation between benign and malignant orbital tumors at 3-T diffusion MR-imaging. *Neuroradiology* 2011;53(7):517-522.

2 Miller NR. Diffusion tensor imaging of the visual sensory pathway: are we there yet? *Am J Ophthalmol* 2005;140(5):896-897.

3 Assaf Y, Pasternak O. Diffusion tensor imaging (DTI)-based white matter mapping in brain research: a review. *J Mol Neurosci* 2008;34(1):51-61.

4 Chanraud S, Zahr N, Sullivan EV, Pfefferbaum A. MR diffusion tensor imaging: a window into white matter integrity of the working brain. *Neuropsychol Rev* 2010;20(2):209-225.

5 Parekh MB, Carney PR, Sepulveda H, Norman W, King M, Mareci TH. Early MR diffusion and relaxation changes in the parahippocampal gyrus precede the onset of spontaneous seizures in an animal model of chronic limbic epilepsy. *Exp Neurol* 2010;224(1):258-270.

6 Wheeler-Kingshott CA, Trip SA, Symms MR, Parker GJ, Barker GJ, Miller DH. *In vivo* diffusion tensor imaging of the human optic nerve: pilot study in normal controls. *Magn Reson Med* 2006;56(2):446-451.

7 Xie S, Gong GL, Xiao JX, Ye JT, Liu HH, Gan XL, Jiang ZT, Jiang XX. Underdevelopment of optic radiation in children with amblyopia: a tractography study. *Am J Ophthalmol* 2007;143(4):642-646.

8 Garaci FG, Bolacchi F, Cerulli A, Melis M, Spanò A, Cedrone C, Floris R, Simonetti G, Nucci C. Optic nerve and optic radiation neurodegeneration in patients with glaucoma: *in vivo* analysis with 3-T diffusion-tensor MR imaging. *Radiology* 2009;252(2):496-501.

9 Wang MY, Qi PH, Shi DP. Diffusion tensor imaging of the optic nerve in subacute anterior ischemic optic neuropathy at 3T. *AJNR Am J Neuroradiol* 2011;32(7):1188-1194.

10 Retracted: changes of radial diffusivity and fractional anisotopy in the optic nerve and optic radiation of glaucoma patients. *Sci World J* 2016;2016:5803036.

11 Li M, Li J, He H, Wang Z, Lv B, Li W, Hailla N, Yan F, Xian J, Ai L. Directional diffusivity changes in the optic nerve and optic radiation in optic neuritis. *Br J Radiol* 2011;84(1000):304-314.

12 Jenabi M, Peck KK, Young RJ, Brennan N, Holodny AI. Identification of the corticobulbar tracts of the tongue and face using deterministic and probabilistic DTI fiber tracking in patients with brain tumor. *AJNR Am J Neuroradiol* 2015;36(11):2036-2041.

13 Bassi L, Ricci D, Volzone A, *et al*. Probabilistic diffusion tractography of the optic radiations and visual function in preterm infants at term equivalent age. *Brain* 2008;131(Pt 2):573-582.

14 Song SK, Sun SW, Ju WK, Lin SJ, Cross AH, Neufeld AH. Diffusion tensor imaging detects and differentiates axon and myelin degeneration in mouse optic nerve after retinal ischemia. *Neuroimage* 2003;20(3):1714-1722.

15 Sun SW, Liang HF, Le TQ, Armstrong RC, Cross AH, Song SK. Differential sensitivity of *in vivo* and ex vivo diffusion tensor imaging to evolving optic nerve injury in mice with retinal ischemia. *Neuroimage* 2006;32(3):1195-1204.

16 Trip SA, Wheeler-Kingshott C, Jones SJ, Li WY, Barker GJ, Thompson AJ, Plant GT, Miller DH. Optic nerve diffusion tensor imaging in optic neuritis. *Neuroimage* 2006;30(2):498-505.

17 Naismith RT, Xu J, Tutlam NT, Trinkaus K, Cross AH, Song SK. Radial diffusivity in remote optic neuritis discriminates visual outcomes. *Neurology* 2010;74(21):1702-1710.

18 Sidek S, Ramli N, Rahmat K, Ramli NM, Abdulrahman F, Tan LK. Glaucoma severity affects diffusion tensor imaging (DTI) parameters of the optic nerve and optic radiation. *Eur J Radiol* 2014;83(8):1437-1441.

19 Schoth F, Burgel U, Dorsch R, Reinges MH, Krings T. Diffusion tensor imaging in acquired blind humans. *Neurosci Lett* 2006;398(3):178-182.

20 Zhong YF, Tang ZH, Qiang JW, Wu LJ, Wang R, Wang J, Jin LX, Xiao ZB. Changes in DTI parameters in the optic tracts of macaque monkeys with monocular blindness. *Neurosci Lett* 2017;636:248-253.

21 Behrens TE, Berg HJ, Jbabdi S, Rushworth MF, Woolrich MW. Probabilistic diffusion tractography with multiple fibre orientations: what can we gain? *Neuroimage* 2007;34(1):144-155.

22 Behrens TE, Woolrich MW, Jenkinson M, Johansen-Berg H, Nunes RG, Clare S, Matthews PM, Brady JM, Smith SM. Characterization and propagation of uncertainty in diffusion-weighted MR imaging. *Magn Reson Med* 2003;50(5):1077-1088.

23 Parker GJ, Haroon HA, Wheeler-Kingshott CA. A framework for a streamline-based probabilistic index of connectivity (PICo) using a structural interpretation of MRI diffusion measurements. *J Magn Reson Imaging* 2003;18(2):242-254.

24 Li Z, Peck KK, Brennan NP, Jenabi M, Hsu M, Zhang Z, Holodny AI, Young RJ. Diffusion tensor tractography of the arcuate fasciculus in patients with brain tumors: comparison between deterministic and probabilistic models. *J Biomed Sci Eng* 2013;6(2):192-200.

25 Beaulieu C. The basis of anisotropic water diffusion in the nervous system - a technical review. *NMR Biomed* 2002;15(7-8):435-455.

26 Thiessen JD, Zhang Y, Zhang H, Wang L, Buist R, Del Bigio MR, Kong J, Li XM, Martin M. Quantitative MRI and ultrastructural examination of the cuprizone mouse model of demyelination. *NMR Biomed* 2013;26(11):1562-1581.

27 Douglas PK, Gutman B, Anderson A, Larios C, Lawrence KE, Narr K, Sengupta B, Cooray G, Douglas DB, Thompson PM, McGough JJ, Bookheimer SY. Hemispheric brain asymmetry differences in youths with attention-deficit/hyperactivity disorder. *Neuroimage Clin* 2018;18:744-752.

28 Glasel H, Leroy F, Dubois J, Hertz-Pannier L, Mangin JF, Dehaene-Lambertz G. A robust cerebral asymmetry in the infant brain: the rightward superior temporal sulcus. *Neuroimage* 2011;58(3):716-723.

29 Zhao L, Herman JE, Patel PK. The structural implications of a unilateral facial skeletal cleft: a three-dimensional finite element model approach. *Cleft Palate Craniofac J* 2008;45(2):121-130.